

Kinetics of fluorine evolution reaction on carbon anodes: influence of the surface C–F films

H. Groult*, S. Durand-Vidal, D. Devilliers, F. Lantelme

Laboratoire LI2C - Électrolytes et Electrochimie, Université Pierre & Marie Curie,
CNRS UMR 7612, 4 Place Jussieu, 75252 Paris Cedex 05, France

Received 22 May 2000; received in revised form 12 June 2000; accepted 26 June 2000

Abstract

During the fluorine evolution reaction by electrolysis of molten KF–2HF, a thin solid fluoro-carbon layer is formed on carbon anodes. This film is mainly composed of fluorine–graphite intercalation compound and a small amount of insulating graphite fluorides. Impedance measurements performed in mercury and cyclic voltammetry studies in aqueous solution containing a redox couple have shown that the surface film behaves like an electronic conductor and cannot constitute a high energy barrier for the electron transfer in electrochemical reactions. However, the kinetics of the fluorine evolution reaction is strongly dependent on the water content in KF–2HF, indeed, water contributes to the formation of graphite fluorides which limit the fluorine evolution reaction. STM measurements performed on crude and passivated highly oriented pyrolytic graphite (HOPG) samples have pointed out the heterogeneities of composition of this carbon–fluorine film and the influence of water. It has been shown that, if the passivation of the carbon electrodes was performed in molten KF–2HF containing a high amount of water, the hexagonal symmetry of the images obtained with HOPG is lost. © 2001 Elsevier Science B.V. All rights reserved.

Keywords: Fluorine; KF–2HF; Carbon; STM.

1. Introduction

The chemical reaction of fluorine with graphite or carbon at high temperature ($350^{\circ}\text{C} < T < 600^{\circ}\text{C}$) leads to the formation of graphite fluorides [1], denoted CF_x in the literature, with covalent C–F bonds. In the formula, x represents the mean stoichiometric coefficient. The composition strongly depends on the temperature of the reaction. Indeed, lower temperatures favour the generation of $\text{CF}_{0.5}$, whereas CF is produced around 600°C . However, the reaction rate of fluorine gas with carbonaceous materials drastically decreases at temperatures less than 300°C .

Solid carbon–fluorine compounds can also be obtained at lower temperature ($T < 100^{\circ}\text{C}$) [2]. These compounds, called fluorine–graphite intercalation compounds (GICs), are obtained by the chemical reaction of fluorine with carbon or graphite in presence of a suitable catalyst. For example, fluorine is intercalated into graphite in presence of gaseous hydrogen fluoride and leads to the formation of $\text{C}_x(\text{HF})_y\text{F}$ with $2 < x < 5$. In presence of metal fluorides, MF_2 , C_xF

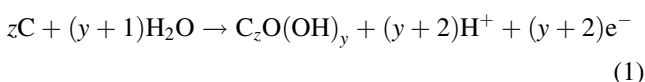
compounds are synthesised. In these compounds, the C–F bonds are semi-ionic or ionic.

The oxidation of carbon in molten KF–2HF ($85^{\circ}\text{C} < T < 100^{\circ}\text{C}$) during the fluorine evolution reaction also gives rise to the formation of a GIC, with a composition of $\text{C}_x(\text{HF})_y\text{F}$, and a small amount of graphite fluorides, CF_x , at the electrode/electrolyte interface [3]. The high anodic overvoltage ($\approx 3\text{ V}$) which characterises this process is attributed to the presence of such a heterogeneous passivated carbon–fluorine film on carbon anodes. Qualitative evidence of the formation of the passivating layer was given by mass spectroscopy [4] and XPS studies [5,6]. Recently, the electronic properties of the carbon–fluorine film formed at the surface of the carbon anode were investigated [7]. We have shown that the surface film behaves like an electronic conductor and cannot constitute a high energy barrier for the electron transfer in electrochemical reactions. The partial inhibition of the fluorine evolution reaction may be explained by the low surface energy of the film, which repels the electrolyte from the electrode. Moreover, it gives rise to lenticular and strongly adherent fluorine bubbles to the surface. However, depending on the chemical composition of the surface film, the

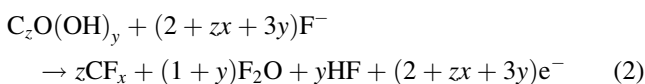
* Corresponding author. Tel.: +33-1-4427-3534; fax: +33-1-4427-3856.
E-mail address: groult@ccr.jussieu.fr (H. Groult).

electrochemical properties are very different. For example, the activation of carbon anodes [6] enhances the detachment of fluorine bubbles owing to a smoothing of the carbon surface. The same modification can also be obtained by doping the carbon electrode with a suitable metallic agent prior to electrolysis [5,8].

For the industrial preparation of fluorine by electrolysis of KF–2HF, one of the most important parameters is the water content in the melt. In presence of water, O₂, CO, CO₂, COF₂ and F₂O evolve in the anodic compartment. Moreover, graphite oxides are formed [1] at about 3 V according to the following reaction



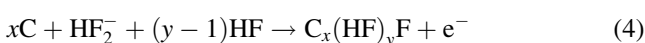
At higher potentials, oxygen in graphite oxide, C_zO(OH)_y, may be easily exchanged with fluorine giving rise to the formation of insulating graphite fluoride [1]



This reaction is concomitant with the formation of fluorine gas which is described by the following half cell reaction



Reaction (3) cannot take place on graphite fluorides because of their insulating properties. It occurs only on the parts of the electrode resulting from the electrofluorination of carbon. On those parts, HF₂⁻ species are electrochemically intercalated into the carbon lattice according to



In these C_x(HF)_yF–GICs, the positive charge is delocalized on *x* carbons. Moreover, this compound is well known to be conductive and wetted by KF–2HF [1].

The influence of water content in molten KF–2HF on the kinetics rate of the fluorine evolution reaction was never clearly pointed out. The aim of this paper is to study that point.

Experiments on the electrochemical behaviour of several kinds of fluorinated carbons were carried out: (i) in molten KF–2HF in a large potential-range in order to study the fluorine evolution reaction; (ii) in aqueous solution containing a redox couple; (iii) in mercury for studying their electronic properties.

The electrochemical experiments were coupled with surface analysis techniques such as X-ray photoelectron spectroscopy (XPS) and scanning tunnelling microscopy (STM) in order to establish correlation between the electrochemical behaviour and the composition of the samples.

The exploitation of all these results provides a better understanding of the influence of the surface fluorinated film on the mechanism involved in the KF–2HF electrolysis.

2. Experimental

Most details of the experimental procedure were described previously [3,5]. Briefly, for the experiments in KF–2HF, a Cu/CuF₂ reference electrode and a graphite counter-electrode were used. The *I*–*E* curves were obtained with an EG&G PAR model 273 generator in a large potential range with a linear potential sweep measurement (*v* = 0.4 V s⁻¹). The anodic material was P2J non-graphitised carbon for fluorine production, manufactured by SGL, France.

Cyclic voltammograms in aqueous medium (1 M KCl containing 10⁻² M K₃Fe(CN)₆/K₄Fe(CN)₆) were performed with an EG&G PAR model 273 generator.

Impedance measurements in mercury were done in the 13 MHz–5 Hz frequency range with a Hewlett-Packard 4192A frequency response analyser driven by a Hewlett-Packard 9816 microcomputer. The amplitude of the sinusoidal perturbation was 10 mV peak-to-peak. No potential was applied between the two electronic conductors (carbon and mercury) in order to study only the electronic properties of the surface films. The cell used for impedance measurements in “dry” conditions is described in [7].

XPS measurements were done with a VG Scientific ESCALAB Mark II spectrometer under ultrahigh vacuum conditions. Mg Kα excitation source was used with a power of 300 W. Copper and gold at the binding energies BE = 932.7 eV for Cu2p_{3/2} and BE = 83.9 eV for Au4f_{7/2} were chosen for the calibration of the spectrometer. The analyser was operating at 20 eV pass energy for high resolution spectra of C1s core level and 50 eV for survey spectra. The analysed area was 10 mm².

STM measurements were carried out with pure cleaved HOPG. Then, the sample was introduced into the electrochemical cell and passivated in KF–2HF at 6 V during 30 min. Two water content in KF–2HF were studied: 20 and 600 ppm. Then, the fluorinated HOPG samples were treated at room temperature under vacuum for one day for removing traces of HF. Nanoscope III and Pt/Ir tips from Digital Instruments were used for the STM analysis in air. The STM images were collected in constant-height mode with small bias voltage (20 mV) and an approach current (setpoint) of 4 nA.

Hereafter, the different samples are numbered as follows:

1. Sample A: platinum electrode.
2. Sample B1: P2J carbon before electrochemical passivation in KF–2HF.
3. Sample B2: HOPG before electrochemical passivation in KF–2HF.
4. Sample C1: P2J passivated in KF–2HF with a water content of: C_{H₂O} < 20 ppm.

5. Sample C2: HOPG passivated in KF–2HF with a water content of: $C_{H_2O} < 20$ ppm.
6. Sample D1: P2J carbon passivated in KF–2HF with a water content of: $C_{H_2O} \approx 600$ ppm.
7. Sample D2: HOPG passivated in KF–2HF with a water content of: $C_{H_2O} \approx 600$ ppm.
8. Sample E1: P2J carbon fluorinated with fluorine gas.
9. Sample E2: HOPG fluorinated with fluorine gas.
10. Sample F: $CF_{0.65}$ (Cefbon-DM[®], Central Glass) prepared from artificial graphite powder.

The electrochemical passivation in KF–2HF was performed by means of a potential sweep between 3 and 6 V, at $\nu = 0.4 \text{ V s}^{-1}$.

The chemical fluorination process for Samples E1 and E2 was carried out in a furnace at 275°C during three hours under pure fluorine atmosphere ($p_{F_2} = 1 \text{ atm}$). Such temperature, pressure and time reaction were chosen in order to obtain a rapid fluorination of the surface of the samples.

3. Results and discussion

3.1. Electrochemical behaviour

I–*E* curves obtained in dehydrated KF–2HF ($C_{H_2O} < 20$ ppm) with Samples A, B1, and E1 are presented in Fig. 1. In the case of crude carbon (Sample B1), the fluorine evolution reaction takes place (leading to Sample C1) with a high anodic overvoltage. Better results were obtained with platinum electrode. For the latter, spherical bubbles are formed [1]; it induces an improvement of the fluorine bubbles detachment and an increase of the electroactive

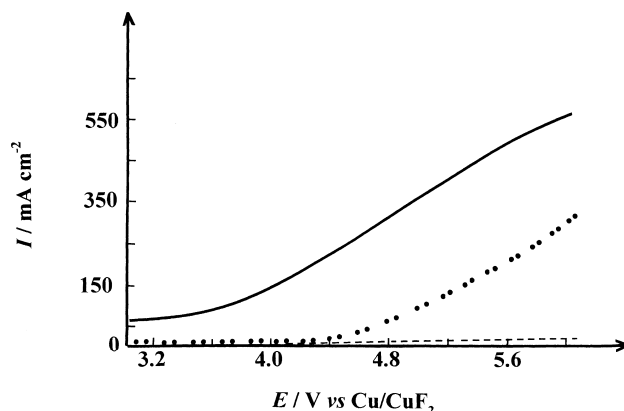


Fig. 1. *I*–*E* curves ($\nu = 0.4 \text{ V s}^{-1}$) obtained in KF–2HF (water content < 20 ppm) at 90°C : (—) Sample A; (●) Sample B1 (leading to Sample C1); (---) Sample E1.

surface area. For Sample E1, the reaction is completely blocked even at high potential.

In order to understand the different behaviours observed with Samples C1 and E1, another sets of experiments were done.

At first, the electron transfer rate of the $Fe^{III/II}$ redox couple in aqueous KCl solution was studied by cyclic voltammetry ($\nu = 20 \text{ mV s}^{-1}$). A platinum working electrode (Sample A) was tested as reference material (Fig. 2). The potential difference, ΔE_p , between anodic and cathodic peaks is about 70 mV. It indicates that the electron transfer kinetics is rapid. Rather similar ΔE_p values are obtained with Samples B1 (90 mV) and C1 (110 mV). By contrast, higher values are observed for Samples D1 (180 mV) and E1 (205 mV). For the two latter, the presence of water in

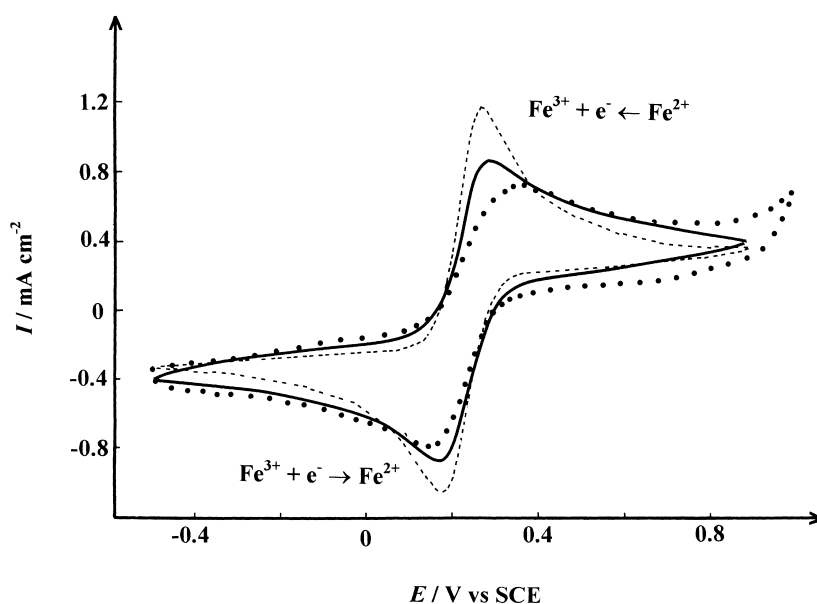


Fig. 2. Cyclic voltammograms ($\nu = 20 \text{ mV s}^{-1}$) obtained in $1 \text{ M KCl} + 10^{-2} \text{ M K}_3\text{Fe}(\text{CN})_6/\text{K}_4\text{Fe}(\text{CN})_6$. (---) Sample A; (—) Sample C1; (●) Sample E1.

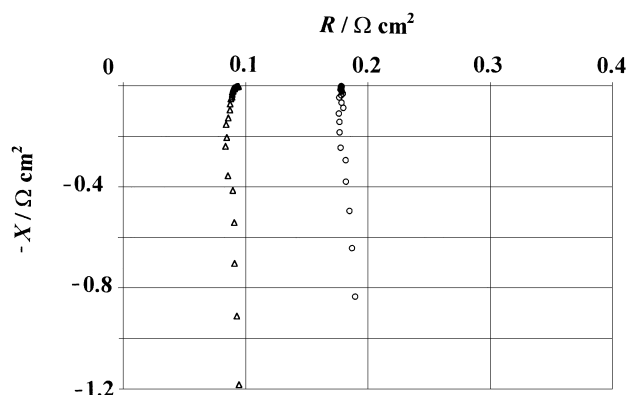


Fig. 3. Impedance diagrams obtained in mercury. (Δ) Sample C1; (\circ) Sample E1.

KF–2HF of the chemical fluorination using fluorine gas give rise to the formation of a more resistive surface layer. However, the electron transfer for the $\text{Fe}^{\text{III/II}}$ redox couple is not blocked with Sample E1 as observed above in KF–2HF for the HF_2^-/F_2 couple.

Impedance measurements performed in mercury [7] led to similar conclusions. Whatever the preparation mode for the fluorination of the carbon electrodes, the Nyquist diagrams (Fig. 3) do not exhibit any capacitive loop. In spite of the presence of the fluorinated surface layer, only an inductive contribution attributed to the wires, and a resistive contribution, R_{HF} , attributed to the ohmic resistance of the material and the surface film, were observed. For Samples C1 and E1, the values of R_{HF} are 0.096 and 0.184 $\Omega \text{ cm}^2$, respectively. The shape of the Nyquist diagrams indicates that the electrons can be transferred from Hg to the carbon substrate and vice versa, i.e. the surface film exhibits electronic conductivity.

The fluorination of carbon during electrolysis of hydrated KF–2HF and by the chemical reaction with fluorine gas gives rise to the formation of more resistive surface film. Indeed, the value of R_{HF} obtained with Sample E1 is larger than that obtained with Sample C1. It explains why the ΔE_p value for Sample E1 is also about two times higher than that obtained with Sample C1. That means that the electron transfer rate for the $\text{Fe}^{\text{III/II}}$ redox couple in KCl is slower.

In conclusion to that section, whatever the preparation mode of the fluorinated surface film on carbon anodes, the film behaves like an electronic conductor, as proposed recently [7]. It does not constitute a high energy barrier for the electronic transfer for the fluorine evolution reaction. The increase of the R_{HF} and ΔE_p values obtained with Samples D1 and E1 may be explained by the presence of a larger amount of CF_x on the surface. For Sample D1, graphite fluorides are formed according to reactions (1) and (2); for Sample E1, graphite fluorides are formed according to



Table 1

Results of XPS investigations for crude and passivated carbon samples^a

Peaks	Samples			
	B1	C1	E1	F
C1s	284.3	284.4	285.6	291.6
F1s	–	688.6 ^b	689.3 ^b	691.9 ^c

^a Values of the binding energy, BE (eV), for the C1s and F1s peaks.

^b Ionic and/or semi-ionic C–F bonds.

^c Covalent C–F bonds.

The CF_x compounds are well known to limit the wettability of the electrode by KF–2HF and locally the electron transfer. Therefore, they are partially responsible for the high value of the anodic overvoltage observed during the fluorine evolution reaction.

Correlations can be established with XPS spectra obtained with the same fluorinated carbon samples.

3.2. XPS investigations

The binding energies for C1s and F1s peaks are given in Table 1.

Similar survey spectra were obtained with all the fluorinated samples. For example, the survey spectrum of Sample E1 is presented in Fig. 4a. It displays C1s, F1s and O1s photoelectron peaks and the characteristic oxygen and fluorine Auger peaks, denoted O(A) and F(A) which result from a de-excitation process.

For Sample C1, the photoelectron peak C1s is situated at 284.4 eV [1,5,6,9] as for crude carbon (Sample B1). Moreover, the F1s region is composed of one peak at 688.6 eV due to semi-ionic C–F bonds [1,5,6,9].

In the case of a chemical fluorination (Sample E1), the peaks corresponding to the C1s and F1s regions are slightly shifted toward higher binding energy values (Table 1). This phenomenon, called “charge effect”, is observed with insulating compounds. However, one can notice that the chemical shift observed for Sample E1 is very small compared to that observed for pure $\text{CF}_{0.65}$ graphite fluorides (Sample F). It confirms the results presented in Section 3.1: the solid carbon–fluorine compound formed at the surface of carbon anodes during the fluorine evolution process in dehydrated KF–2HF is a good conductor.

The F1s region of Sample E1 (Fig. 4b) is composed of two contributions at 689.3 and 692.8 eV due to semi-ionic and covalent C–F bonds [1,10], respectively. The reaction of fluorine gas on carbon at $T < 300^\circ\text{C}$ (leading to Sample E1) gives rise to soft fluorination. It induces the formation of fluorine–GIC with ionic and/or semi-ionic C–F bonds and insulating graphite fluorides, CF_x , with covalent C–F bonds. In Sample E1, the amount of graphite fluorides is higher than that in Sample C1. The presence of these CF_x have a small influence on the results obtained by impedance measurements in mercury or on the cyclic voltammograms

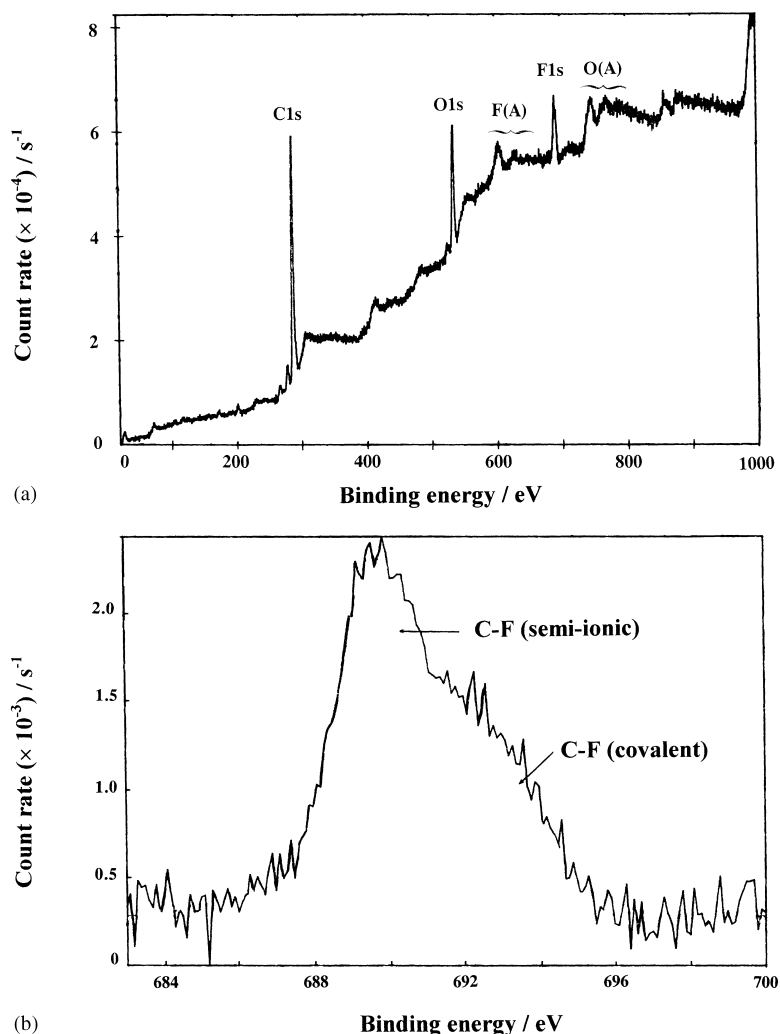


Fig. 4. XPS analysis: (a) survey spectrum of Sample E1; (b) high resolution spectrum of the F1s region of Sample E1.

performed in aqueous solution in term of electronic conductivity. By contrast, as shown in Fig. 1, they have a great influence on the electrochemical behaviour of the carbon anode in KF–2HF during fluorine evolution process since they limit drastically the wettability of the electrode by the melt.

In order to point out the heterogeneities of composition on the surface of passivated carbon electrodes, surface analysis by STM were performed. This technique is a suitable tool for the determination of the local atomic-scale surface structure. These experiments were carried out with crude (Sample B2) and fluorinated HOPG (Samples C2, D2 and E2).

3.3. STM measurements

All the experiments were performed with the constant height mode in air.

The STM images of pure HOPG (Sample B2) after cleavage (Fig. 5a) present typical hexagonal symmetry, in

agreement with the literature [11]. Only half of the carbon atoms of a graphene layer exhibit high electronic density, due to the non-equivalence of the atomic sites resulting from the ABAB stacking of graphene layers.

In the case of HOPG samples electrochemically fluorinated in dehydrated KF–2HF (Sample C2), in many parts of the surface the approach of the tip cannot be done since no current was detected, even for high bias values. In those parts of the electrode, graphite fluorides were present [7]. However, in most parts of the electrode, conducting GIC is formed according to reaction (4); the same hexagonal symmetry (Fig. 5b) as that of HOPG was observed, with a periodicity of 0.244 nm. An overlap of the electronic densities between two neighbouring atoms was observed due probably to the formation of C–F bonds which modify the electronic densities of each carbon atom [7].

If the electrochemical fluorination is performed in KF–2HF containing $\text{C}_2\text{H}_2\text{O} \approx 600$ ppm (Sample D2), insulating

graphite fluorides are present on the electrode. The approach of the tip cannot be done since no current was detected, even for high bias values. Conducting areas are also detected. Nevertheless, the hexagonal structure of HOPG is completely lost as illustrated in Fig. 5c.

In the case of chemical fluorination (Sample E2), a modification of the hexagonal structure of the starting material was also pointed out (Fig. 5d). It is reported [1]

that during the formation of graphite fluorides at $T > 350^\circ\text{C}$, a new structure with the chair-structure of cyclohexane in which the chemical bond was completely changed to sp^3 is observed [1]. In our case, because of the temperature of the reaction ($T = 275^\circ\text{C}$), one can assume that the images observed with Sample E2 correspond to an intermediate step between the hexagonal symmetry of pure HOPG and the structure of graphite fluorides.

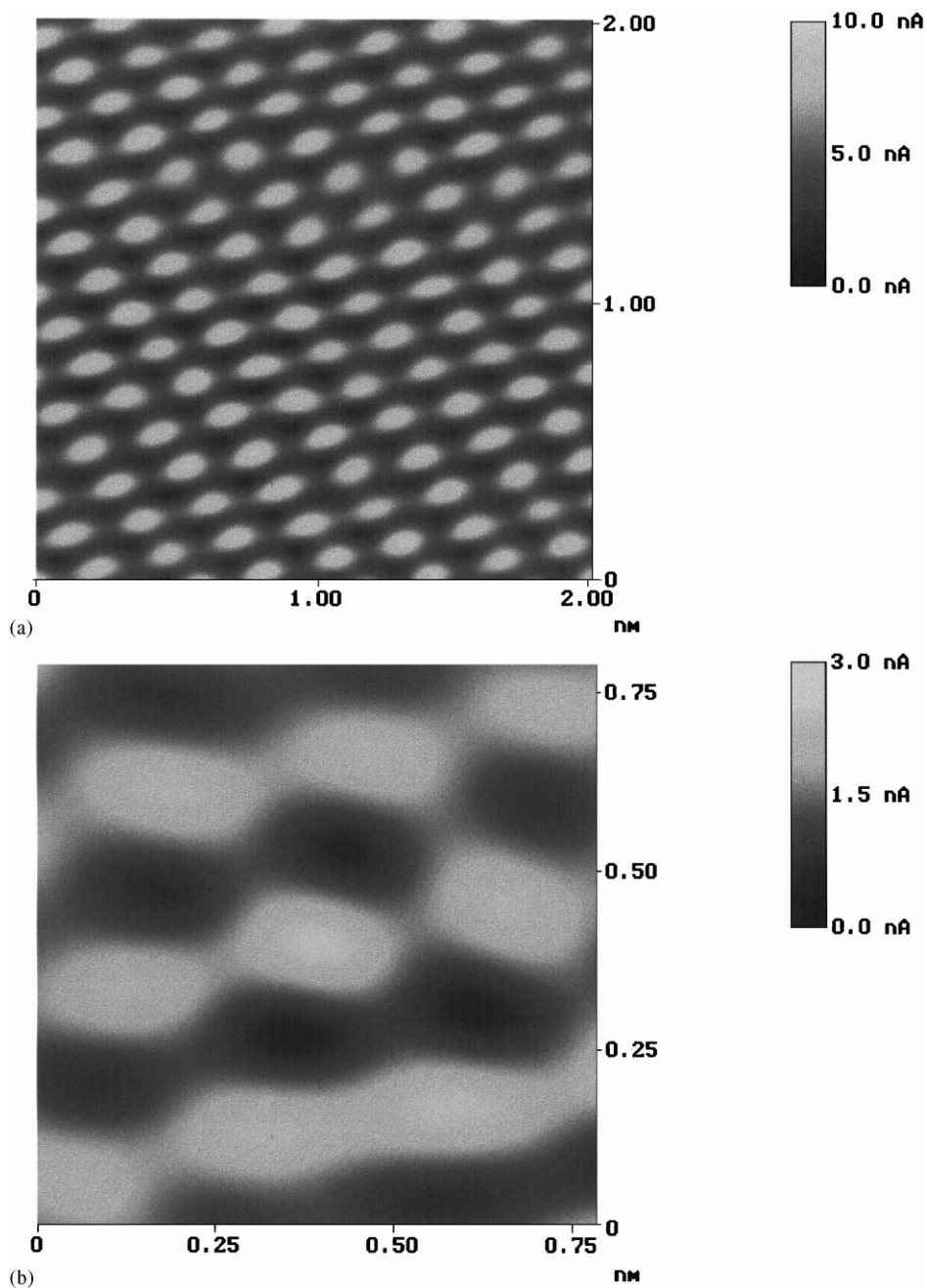


Fig. 5. (a) STM image for Sample B2. Experimental conditions: bias voltage: 20 mV; setpoint: 5 nA; z range: 10 nA. (b) STM image for Sample C2. Experimental conditions: bias voltage: 20 mV; setpoint: 4 nA; z range: 3 nA. (c) STM image for Sample D2. Experimental conditions: bias voltage: 15 mV; setpoint: 5 nA; z range: 5 nA. (d) STM image for Sample E2. Experimental conditions: bias voltage: 20 mV; setpoint: 5 nA; z range: 5 nA.

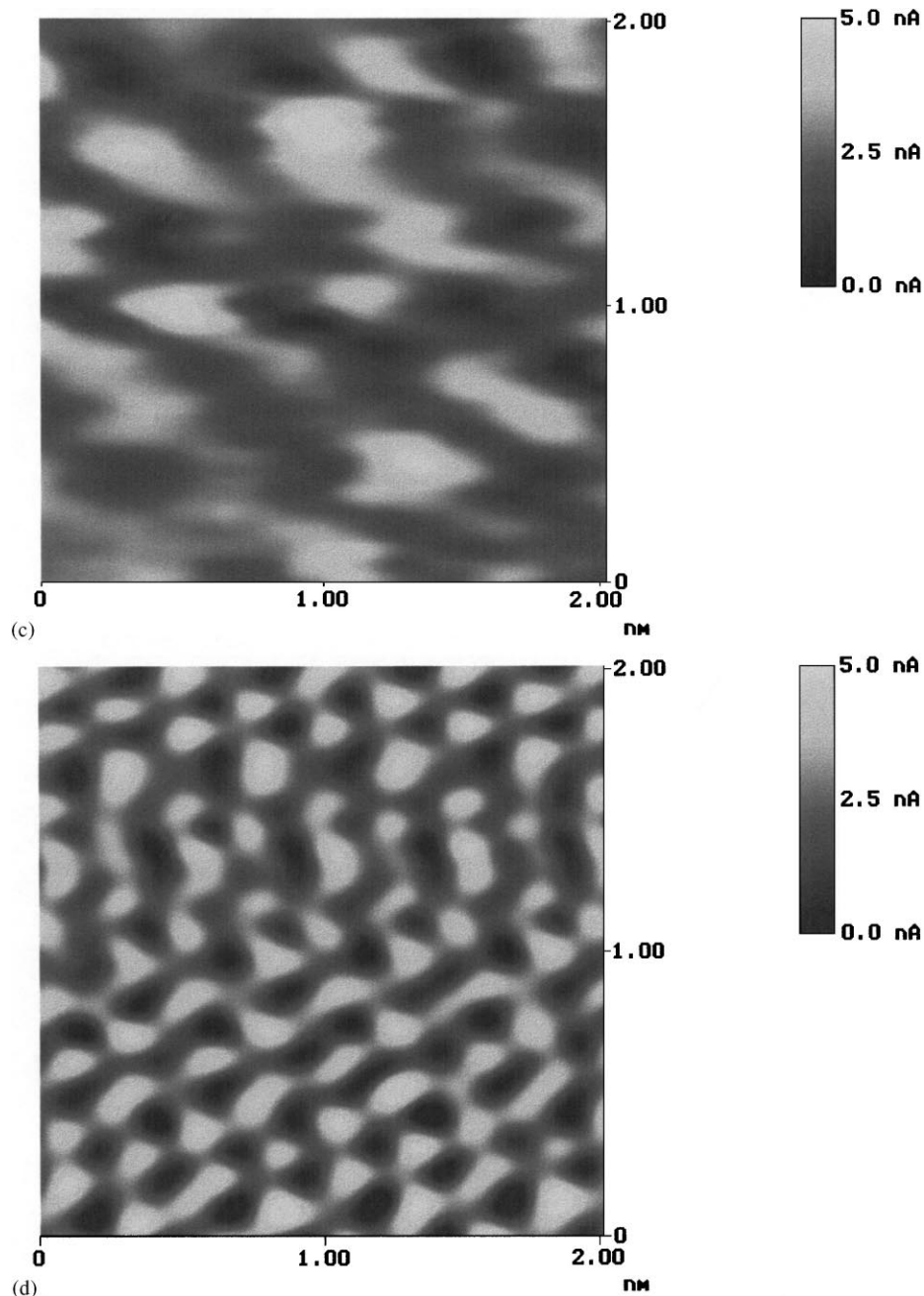


Fig. 5. (Continued).

4. Conclusion

A solid carbon–fluorine film is formed on carbon anodes during electrolysis of molten KF–2HF or by chemical fluorination using fluorine gas. This film is composed of conducting GIC and a small amount of graphite fluorides. The amount of graphite fluorides is strongly dependent on the water content in KF–2HF. Although their contribution in term of electronic properties of the surface film is low, they have a great influence on the kinetics of the fluorine evolution reaction. Thus, this reaction is completely blocked when

the fluorinated film is prepared in KF–2HF containing large amount of water.

These conclusions were confirmed by XPS and STM investigations. The presence of fluorine–GICs was revealed by XPS and STM experiments performed on pure and fluorinated carbon samples. In the case of electrochemical fluorination in a dehydrated KF–2HF melt, the hexagonal symmetry of the HOPG is kept. By contrast, if the melt contains a high amount of water, the hexagonal symmetry of the starting material seems to be completely destroyed.

Therefore, the high anodic overvoltage may be related to the graphite fluorides present on the surface of the electrode which repel the electroactive species from that surface.

Acknowledgements

Grateful acknowledgements are made to Dr. C. Hinnen (Laboratoire de Physicochimie des Surfaces, E.N.S.C.P., Paris) for performing XPS measurements and to the Comurhex-Cogema Company (Pierrelatte) for their joint-support of this research project.

References

- [1] N. Watanabe, T. Nakajima, H. Touhara, Graphite Fluorides, Elsevier, Amsterdam, 1988 (Chapter 1).
- [2] T. Nakajima, N. Watanabe, Graphite Fluorides and Carbon–Fluorine Compounds, CRC Press, Boca Raton, FL, 1991 (Chapter 6).
- [3] H. Groult, D. Devilliers, M. Vogler, Current Topics in Electrochemistry, Research trends, Vol. 4, Poojapura, Trivandrum, India, 1997, p. 23.
- [4] D. Devilliers, M. Vogler, F. Lantelme, M. Chemla, Anal. Chim. Acta 153 (1983) 69–82.
- [5] H. Groult, D. Devilliers, M. Vogler, C. Hinnen, P. Marcus, F. Nicolas, Electrochim. Acta 38 (1993) 2413.
- [6] L. Bai, B.E. Conway, J. Appl. Electrochem. 20 (1990) 925.
- [7] H. Groult, D. Devilliers, S. Durand-Vidal, F. Nicolas, M. Combet, Electrochim. Acta 44 (1999) 2793.
- [8] T. Tojo, J. Hiraiwa, M. Dohi, Y. Chong, J. Fluorine Chem. 57 (1992) 93.
- [9] L. Bai, B.E. Conway, J. Appl. Electrochem. 20 (1990) 916.
- [10] H. Groult, D. Devilliers, M. Vogler, P. Marcus, F. Nicolas, J. Electrochem. Soc. 144 (1997) 3361.
- [11] R. Wiesendanger, D. Anselmetti, in: H.-J. Güntherodt, R. Wiesendanger (Eds.), Scanning Tunnelling Microscopy, Springer, Berlin, Vol. 1, 1992, p. 131.